JOURNAL OF AGRICULTURAL AND FOOD CHEMISTRY

Biflavonoids Isolated from *Selaginella lepidophylla* Inhibit Photosynthesis in Spinach Chloroplasts

María Isabel Aguilar,*,† Maryosawa G. Romero,† María Isabel Chávez,# Beatriz King-Díaz,§ and Blas Lotina-Hennsen§

Departamento de Farmacia, Departamento de Bioquímica, Facultad de Química, and Instituto de Química, Universidad Nacional Autónoma de México, México D.F., C.P. 04510, Mexico

Through bioactivity-guided chemical analysis of *Selaginella lepidophylla*, biflavonoids robustaflavone (**1**), 2,3-dihydrorobustaflavone (**2**), and 2,3-dihydrorobustaflavone-5-methyl ether (**3**) were isolated and their structures confirmed by spectroscopic and spectrometric analyses. Their NMR resonances were unambiguously assigned from HMBC, NOESY, and NOESY-1D experiments, and absolute configurations of **2** and **3** were established. Compound **3** has not been reported, and although structure of **2** was described before, the ^{13}C NMR assignment does not correlate with the structure reported. Therefore, this is the first report of **2**. All compounds inhibited ATP production. Compounds **1** and **2** behaved as Hill reaction inhibitors. **1** interacted with photosystem II, transforming the reaction centers to silent centers at 300 and 600 μM. The interaction and inhibition target of **2** was located on Cyt b_6f to PC. The three compounds also behaved as energy transfer inhibitors, **3** being the most active.

KEYWORDS: 2,3-Dihydrorobustaflavone; 2,3-dihydrorobustaflavone-5-methyl ether; photosynthesis; H^+-ATPase; robustaflavone; *Selaginella lepidophylla*

INTRODUCTION

Selaginella lepidophylla (Hook. & Grey.) Spring (Selaginellaceae), locally known as "resurrection plant", "rose of Jericho", "siempre viva", "flor de piedra", "doradilla", "flower of rock", "stone flower", or "magóra" (tarahumara), is a fern that grows in isolated specimens of up to 20 cm in diameter when extended. This plant is found in the Middle East, in the Central Americas, and in most states of Mexico. It grows particularly in well-drained soils and can stand long periods of drought and heat. As a fern, it does not bloom. It can grow in high-stress conditions, producing secondary metabolites. The whole plant is highly valued in some regions of Mexico as an antimicrobial, being used to treat urinary infections (*1*). Robustaflavone is a potential non-nucleoside antihepatitis B agent (*2*).

In our search for secondary metabolites from plants that affect photosynthesis, we found three biflavonoids, robustaflavone (**1**), 2,3-dihydrorobustaflavone (**2**), and 2,3-dihydrorobustaflavone 5-methyl ether (**3**), considering **2** and **3** as novel compounds. All three compounds inhibited ATP synthesis and several other photosynthetic processes including electron flow, PSII, PSI, and their partial reactions on chloroplasts. These studies were performed by polarographic techniques, corroborated by fluorescence induction curves of chlorophyll *a* of photosystem II (PSII), as shown in the JIP test (*3*).

MATERIALS AND METHODS

General Procedures. UV spectra were obtained on a Shimadzu UV 160; IR spectra were recorded in KBr on a Perkin-Elmer 1605 spectrophotometer; circular dichroisms were measured on a Jasco J-720 polarimeter; ^{1}H NMR and ^{13}C NMR spectra were recorded at 500 and 125 MHz, respectively, on a Varian Inova apparatus; all NMR spectra were recorded in deuterated acetone with TMS as the internal standard. Si gel 60 (0.063−0.200 mesh) Merck and lipophilic Sephadex LH-20 100-50 (25−100 μ) Sigma-Aldrich were used for column chromatography; thin layer chromatography was done on Alugram Sil G/UV$_{254}$ Macherey-Nagel. Low-resolution FAB$^+$ mass spectra were recorded on a JEOL SX model 102-A apparatus.

Plant Material. The whole plant of *S. lepidophylla* was purchased in Mercado de Sonora in Mexico City in August 2005 and was identified by Dr. R. Bye. Reference samples have been deposited at the ethnobotanical collection of the National Herbarium, Instituto de Biología, UNAM.

Extraction and Isolation Procedures. The whole plant of *S. lepidophylla* (1.6 kg) was air-dried at room temperature and pulverized. The total extract (130 g) was obtained by percolation with $CHCl_3$/MeOH (50:50), at room temperature; solvent was evaporated in vacuum at 50 °C. The crude extract (130 g) was suspended in MeOH/H_2O (80:20) and then partitioned successively with hexane, ethyl acetate, and *n*-butanol, yielding 43.7, 11.3, and 8.9 g of each extract, respectively. The EtOAc extract (11 g) was subjected to column chromatography on silica gel 60 (170 g), using for elution mixtures of solvents of increasing polarity, starting with hexane, followed by hexane/EtOAc, EtOAc, $CHCl_3$, $CHCl_3$/MeOH, and MeOH. Fractions were collected in 500 mL portions and combined according to their TLC profile, to

* Author to whom correspondence should be addressed [telephone (22)(55) (56 22 52 90); fax (22)(55) 5622 5329; e-mail laurents@servidor.unam.mx].
† Departamento de Farmacia.
§ Departamento de Bioquímica, Facultad de Química.
# Instituto de Química.

10.1021/jf8010432 CCC: $40.75
Published on Web 07/23/2008

Table 1. Effect of Extracts and Fractions on ATP Synthesis

extracts and fractions	I_{50} (ppm)
$CHCl_3$/MeOH (total)	28
hexane	68
ethyl acetate	38
n-butanol	72
F10	38
FII6	18
FII5	68

afford a total of 14 fractions (F1−F14). Fraction F10 (2 g) was rechromatographed over silica gel 60 using $CHCl_3$/MeOH in mixtures of increasing polarity, starting with $CHCl_3$ (100%) and ending with MeOH (100%). Fractions (300 mL each) were collected and combined according to their similarity by TLC, to yield a total of 7 subfractions (FII1−FII7). FII6 was purified on a lipohilic sephadex column (50 g), eluting with 50 mL portions of MeOH, to give compounds **1** and **3**. From subfraction FII5, treated as FII6, 103 mg of **2** was obtained.

Robustaflavone (**1**): yellow powder; UV (MeOH) 235, 268, 334 nm; IR ν (KBr) 3422, 1651 cm^{-1}; ^1H and ^{13}C NMR, see **Tables 2** and **3**. FAB-MS (pos.): 539 $[M+H]^+$.

2,3-Dihydro-robustaflavone (**2**): yellow powder; UV (MeOH) 223, 287, 331 nm; CD (*c* 0.02, MeOH) $\Delta\varepsilon$ (λ nm) 0 (260), −4.2 (287), 0 (308), +1.5 (331); IR ν (KBr) 3422, 1643, 1609 cm^{-1}; ^1H and ^{13}C NMR, see **Tables 2** and **3**; FAB-MS (pos) 541 $[M + H]^+$.

2,3-Dihydrorobustaflavone 5-methyl ether (**3**): yellow powder; UV (MeOH) 220, 289, 330 nm; CD (*c* 0.01, MeOH) $\Delta\varepsilon$ (λ nm) 0 (265), −2.5 (289), 0 (312), +1.6 (330); IR ν (KBr) 3355, 1725, 1646 cm^{-1}; ^1H and ^{13}C NMR, see **Tables 2** and **3**. FAB-MS (pos) 555 $[M + H]^+$.

Chloroplast Isolation and Total Chlorophyll Determination. Intact chloroplasts were prepared from market spinach leaves (*Spinacea oleraceae* L.) as published (*4, 5*) by homogenization and differential centrifugation and resuspended in a small volume of the following medium: 400 mM sucrose, 5 mM $MgCl_2$, 10 mM KCl, and 30 mM tricine−KOH (pH 8.0). Chlorophyll concentration was determined as reported (*6*).

Measurement of ATP Synthesis. To measure ATP synthesis, intact chloroplasts (20 μg/mL of chlorophyll) were broken by osmotic rupture in nonbuffered solution with 100 mM sorbitol, 10 mM KCl, 5 mM $MgCl_2$, 0.5 mM KCN, 50 μM MV (methylviologen was used as electron acceptor), 1 mM Na^+−tricine (pH 8.0), and 1 mM ADP (pH 6.7); the pH was adjusted to 8.0 with 50 mM KOH, and the mixture was illuminated for 1 min; the synthesized ATP was calculated as micromoles of ATP per milligram of Chl per hour (*7*).

Measurement of the Rate of Noncyclic Electron Transport. Electron flow (basal, phosphorylating, and uncoupled) from water to MV was monitored with a YSI (Yellow Springs Instrument) oxygraph using a Clark electrode (*5, 8*). Light-induced noncyclic electron transport determination was performed in the presence of 50 μM MV. Chloroplasts were efficiently lysed to yield free thylakoids prior to each experiment by incubating them in the following basal electron transport medium: 100 mM sorbitol, 10 mM KCl, 5 mM $MgCl_2$, 0.5 mM KCN, and 30 mM tricine (*N*-tris[hydroxymethyl]methylglicine) buffer (pH 8 with the addition of KOH). Twenty micrograms of chlorophyll per milliliter of medium was illuminated during 1 min. Phosphorylating noncyclic electron transport was measured as basal noncyclic electron transport medium in the addition of 1 mM ADP and 3 mM KH_2PO_4. Uncoupled electron transport was tested in the basal transport medium by adding 6 mM NH_4Cl as uncoupler agent.

Uncoupled PSII and PSI Electron Flow Measurements. These experiments were performed as an uncoupled noncyclic electron transport assay; the activities were monitored with a YSI oxygen monitor, model 5300, using a Clark type electrode. Uncoupled PSII from water to DCPIP was measured by the reduction of DCPIP-supported O_2 evolution. One micromolar 2,5-dibromo-6-isopropyl-3-methyl-1,4-benzoquinone (DBMIB), 100 μM 2,6-dichlorophenol indophenol (DCPIP), 300 μM $K_3[Fe(CN)_6]$, and 6 mM NH_4Cl were added; MV was omitted. Uncoupled partial reaction of PSII electron

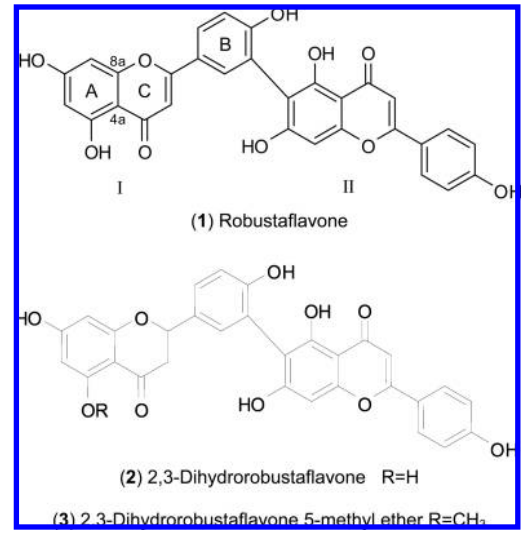

Figure 1. Structures of biflavonoids **1**, **2**, and **3**.

transport from water to sodium silicomolybdate (SiMo) was determined with the basal electron transport medium containing additionally 200 μM SiMo, 10 μM [3-(3,4-dichlorophenyl)-1,1-dimethylurea] (DCMU) (*9*), and 6 mM NH_4Cl; MV was omitted. Uncoupled electron transport from diphenylcarbazide (DPC) to DCPIP was determined in thylakoids (45 μg of Chl) that were previously incubated with 0.8 M Tris, pH 8.0, during 30 min at 4 °C (*11*). Then, the thylakoids were centrifuged at 5000*g* (Sorvall super T21) for 2 min; the pellet was suspended with 500 μL in the reaction medium and was used in the partial PSII reaction from DPC to DCPIP electron flow, assayed spectrophotometrically at 600 nm and quantifying the reduction of DCPIP with the molar extinction coefficient value of 21.8×10^{-3} cm^{-1} mol^{-1} (*10*). The uncoupled PSI electron transport was determined using 3 mL of basal electron transport medium, plus 10 μM DCMU, 100 μM DCPIP, 300 μM ascorbate, and 6 mM NH_4Cl (*12*). The partial reaction of uncoupled PSI from P_{700} to Fx was measured from 100 μM phenylmetasulfate (PMS)/300 μM ascorbate to MV, by the basal electron transport assay using thylakoids poisoned with KCN (an electron transport inhibitor at the plastocyanin level). Chloroplasts suspended in isolated medium were transferred to an ice-chilled test tube containing basal electron transport medium with 30 mM KCN. The test tube was incubated 60 min at 4 °C in the dark. The treatment was finished by dilution with 10 mL of a medium containing 0.1 M sucrose, 30 mM *N*-[2-hydroxyethyl]piperazine-*N*′-[2-ethanesulfonic acid] (HEPES)−NaOH buffer (pH 7.2), and 2 mM $MgCl_2$ (*13*); with this treatment, a stoichiometric release of plastocyanin−Cu from the lamellar membrane exposed to KCN occurs. Then, the thylakoids were centrifuged at 5000*g* (Sorvall super T21) for 2 min. The pellet was suspended with 500 μL of the isolated medium; the chlorophyll concentration was measured according to the method of Strain et al. (*6*). In each assay, 1 μM DBMIB (a b_6f complex inhibitor) and reduced PMS as electrons donator at P_{700} (as was demonstrated by electron paramagnetic resonance (EPR) (*14*)) were added to the basal electron transport medium. Electron flow from tetramethyl-*p*-benzohydroquinone ($TMQH_2$) to MV was determined polarographically. In chloroplasts, tetramethyl-*p*-benzohydroquinone supports high rates of phosphorylation-coupled noncyclic electron flow through photosystem I to methylviologen. The reaction is totally sensitive to dibromothymoquinone, indicating an electron donation to the plastoquinone region of the photosynthetic chain (*15*). The I_{50} values were calculated.

Chlorophyll *a* (Chl *a*) Fluorescence Determinations. Chl *a* fluorescence was measured at room temperature with a Hansatech Fluorescence Handy PEA (plant efficiency analyzer) in 5 min dark-adapted chloroplasts (20 μg/mL) as was previously published by Strasser et al. (*3, 5*). The maximum fluorescence yield from the sample was generated using three red intensity light emitting diodes (broadband 650 nm) of 3000 μmol m^{-2} s^{-1}. The pulse duration was 2 s. To monitor Chl *a* fluorescence transients, aliquots of dark-adapted thylakoids containing 20 μg of Chl were transferred to a filter paper by gravity

Table 2. ^{1}H NMR Data of Compounds **1**−**3** at 500 MHz in CD_3COCD_3 (δ in Parts per Million, J in Hertz; Arbitrary Atom Numbering)

position	1	2	3
2		5.48 (dd, J = 13.0, 3.0)	5.36 (dd, J = 13.0, 3.0)
3	6.55 (s)	2.75 (dd, J = 17.0, 3.0, H_{ax}) 3.22 (*dd*, J = 17.0, 13.0, H_{eq})	2.59 (dd, J = 16.5, 2.5, H_{ax}) 2.99 (*dd*, J = 16.2, 13.2, H_{eq})
6	6.28 (d, J = 2.0)	5.96 (d, J = 2.0)	6.10 (d, J = 2.0)
8	6.14 (d, J = 2.0)	5.93 (d, J = 2.0)	6.04 (d, J = 2.0)
2′	8.32 (d, J = 2.5)	7.39 (br s)	7.43 (d, J = 2.5)
5′	6.91 (d, J = 8.5)	7.00 (dd, J = 8.0, 0.5)	6.97 (d, J = 8.5)
6′	7.77 (dd, J = 8.5, 2.5)	7.38 (dd, J = 8.0, 2.0)	7.35 (dd, J = 8.5, 2.5)
3″	6.49 (s)	6.64 (s)	6.61 (s)
8″	6.07 (s)	6.68 (s)	6.64 (s)
2‴	7.70 (d, J = 9.0)	7.93 (d, J = 8.5)	7.92 (d, J = 9.0)
3‴	6.64 (d, J = 9.0)	7.01 (d, J = 8.5)	7.01 (d, J = 9.0)
5‴	6.64 (d, J = 9.0)	7.01 (d, J = 8.5)	7.01 (d, J = 9.0)
6‴	7.70 (d, J = 9.0)	7.93 (d, J = 8.5)	7.92 (d, J = 9.0)
5-OMe			3.76 (s)
5-OH		12.21 (s)	
5″		13.41	13.46

Table 3. ^{13}C NMR Data of Compounds **1**−**3** at 125 MHz in CD_3COCD_3 (δ in Parts per Million; Arbitrary Atom Numbering)

position	1	2	3	position	1	2	3
2	166.2	80.1	79.9	2″	163.7	165.0	164.7
3	102.9	46.6	46.5	3″	103.3	104.1	104.0
4	182.8	197.3	188.3	4″	182.7	183.2	183.0
4a	104.7	103.2	106.2	4a″	102.8	105.3	104.8
5	163.0	164.5	163.7	5″	156.1	161.0	161.6
6	94.9	95.8	94.0	6″	108.8	110.0	110.5
7	166.2	167.4	165.0	7″	174.0	163.0	164.7
8	99.9	96.8	96.7	8″	103.4	94.7	95.1
8a	158.8	165.3	166.0	8a″	162.3	158.0	158.0
1′	119.2	130.6	130.8	1‴	123.5	123.3	123.4
2′	132.4	132.2	132.2	2‴	128.8	129.2	129.2
3′	125.5	120.5	121.0	3‴	116.7	116.9	116.8
4′	166.0	157.0	157.1	4‴	161.6	161.9	161.8
5′	120.8	117.0	117.3	5‴	116.7	116.9	116.8
6′	126.8	128.4	127.9	6‴	161.6	129.2	129.2
				5-OMe			56.0

and immediately dipped in 3 mL of basal noncyclic electron transport medium with different concentrations of the compounds. Different photosynthetic parameters associated with PSII were obtained according to the equations of the O-J-I-P test using the program Biolyzer (*16*): (1) the absorption of photons (ABS) per reaction center (RC) shows the antenna size estimated by the ratio RC/ABS; (2) the maximal trapping rate of PSII describes the maximal rate by which an excitation is trapped by the RC, TRo/RC = $Mo(1/V_J)$; (3) the electron transport in an active RC, ETo/RC = $Mo(1/V_J)\Psi o$; (4) the slope of the normalized curve at the origin of the fluorescence rise, it is a measure of the rate of the primary photochemistry, Mo or $dV/dt_0 = 4(F_{300} - F_0)/(F_m - F_0)$; (5) the non-photochemical energy dissipation per reaction center, DI_0/RC; (6) the de-excitation constants, photochemical de-excitation constant, Kp = (ABS/CS)Kf[(1/Fo)Area/$(F_m - F_0)(1/F_m)$]; (7) non-photochemical de-excitation constants, Kn summing up K_H (for heat dissipation) and KF (for fluorescence emission), K_n = (ABS/CS)$K_f(1/F_m)$; (8) sum $K = K_p + K_n$ = (ABS/CS)$K_f(1/F_0)$; (9) the normalized area measures the energy needed to close all reaction centers, S_m = area/$(F_m - F_0)$; (10) the trapping probability, or quantum yield efficiency, expresses the probability that an absorbed photon will be trapped by the PSII reaction center, φ_{P0} or TRo/ABS = ($F_m$area/$(F_m - F_0)F_0)/F_m$; (11) the probability that an exciton trapped by the PSII reaction center enters the electron transport chain, Ψo or ETo/TRo = area/$(F_m - F_0)V_J$; (12) quantum yield (at t = 0) of energy dissipation, φ_{E0} = ETo/TRo = $(1 - V_J)$; (13) relative variable fluorescence at the J step, $V_J = (F_J - F_0)/F_m - F_0)$.

Mg^{2+}-ATPase Assays. Chloroplasts were isolated from 30−40 g of spinach leaves, which were ground in 160 mL of medium containing 350 mM sorbitol, 5 mM ascorbic acid, and 20 mM 2-(*N*-morpholino)-ethanesulfonic acid (MES), pH 6.5. Chloroplasts were centrifuged at 3000*g* for 60 s, washed once in 40 mL of grinding medium, and resuspended in 35 mM HEPES, pH 7.6. Light-triggered Mg^{2+}-ATPase activity bound to thylakoid membranes was measured according to the method of Mills et al. (*4*). Released inorganic P was measured as reported Sumner (*17*).

RESULTS AND DISCUSSION

Biflavonoids Isolation and ATP Synthesis Determination. In the screening bioassay of ATP synthesis, performed with the extracts and fractions of *S. lepidophylla*, the ethyl acetate extract gave the greatest inhibition (I_{50} 38 ppm, **Table 1**.) Chromatographic primary fraction F10 from the ethyl acetate extract displayed inhibitory effect with the same I_{50} value as the extract, whereas subfractions FII5 and FII6 inhibited the ATP production at 68 and 18 ppm, respectively. The rest of the fractions displayed minor inhibitory effects. To know the compounds involved in this inhibitory activity, FII6 was purified to give two biflavonoids as yellow powders: robustaflavone (**1**, 130 mg) and 2,3-dihydrorobustaflavone 5-methyl ether (**3**, 14 mg); 2,3-dihydrorobustoflavone (**2**, 300 mg) was purified from FII5. Structures of **1**, **2**, and **3** (**Figure 1**) were elucidated by the analysis of their spectroscopic data; UV and IR indicated their biflavonoid nature. Compounds **1** and **2** have been earlier isolated from several species of *Selaginella*, and their spectroscopic signals were also reported (*18–23*). According to Markham et al. observations (*20*), the three compounds obtained in our work belong to the robustaflavone series, owing to the fact that the interflavonoidal linkage carbon between δ 108 and 110 in ^{13}C NMR was present. In our NMR experiments, use of deuterated acetone instead of DMSO-d_6 led to better resolved spectral signals.

Compound **2** showed three aliphatic ^{1}H NMR resonances at δ 5.48, 3.22, and 2.75, and in combination with a C═O ^{13}C NMR resonance at δ 197.3 (**Tables 2** and **3**), the presence of a flavanone subunit is indicated. Correlations in the HMBC spectrum of this compound were observed between H−C(2) and C(6′) and between CH_2(3) and C(2), C(4), C(1′), and C(4a), and between both H−C(6) and H−C(8) and C(7) and C(4a). It is worth noting the correlations between the hydroxyl group at position 5 of the flavanone unit as H−O(5) and C(4a), C(5), C(6), which settled the position of C-5 at 165.0 ppm. In ring B of this same unit correlations were observed between H−C(2′) and C(4′), C(6″), C(6′), and C(2), between H−C(5′) and C(4′), C(1′), and C(3′), and between H−C(6′) and C(4′), C(2), and C(2′). In subunit II, correlations were observed between H−C(3″), C(2″), C(4″), and C(4″a), between H−C(8″) and C(8″a), C(4″a), C(6″), and C(7″), and between H−O(5″) and the quaternary carbon 6″, C(4″a), and C(5″), in the flavone unit.

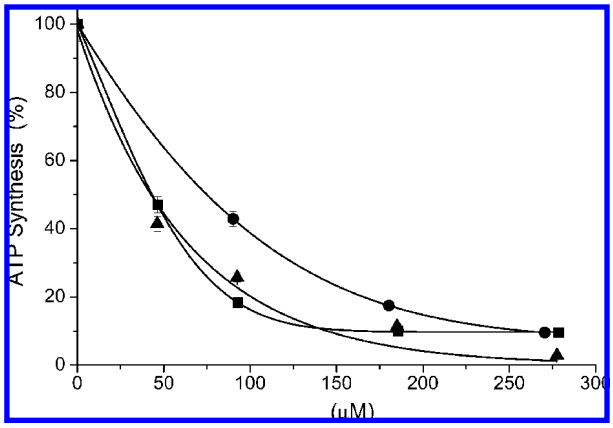

Figure 2. Effect of biflavonoids on ATP synthesis: robustaflavone (**1**) (■); 2,3-dihydrorobustaflavone (**2**) (●); 2,3-dihydrorobustaflavone 5-methyl ether (**3**) (▲). Control = 100% = 630 μM ATP/mg of Chl/h. Results are the average of three replicates.

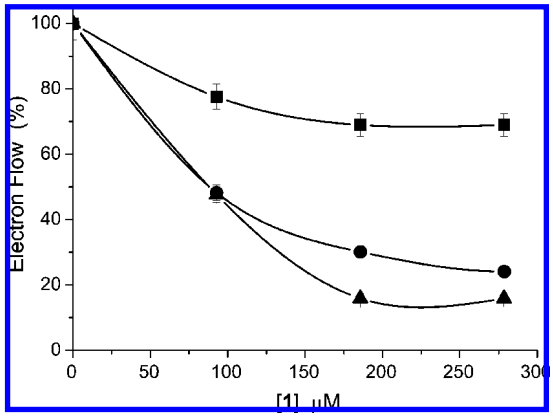

Figure 3. Effect of robustaflavone (**1**) on electron transport flow: basal (■); phosphorylating (●); uncoupled (▲). Control = 100% = 387, 553, and 1420 μequiv of e^-/mg of Chl/h, respectively. Each curve is the average of three replicates.

The interflavonoidal linkage was established through the HMBC correlation between H−C(2′) and C(6″). Moreover, as above-mentioned, this last carbon (C-6″) correlates with the hydroxyl hydrogen at C(5″) and with H−C(8″). The signal for C(6″) was found at 110 ppm. Both ^{1}H and ^{13}C NMR data of **2** are depicted in **Tables 2** and **3**. Recently, Bahia and co-workers assigned the structure of **2** for a compound they isolated from *Caesalpinia pyramidalis* (*23*). However, we observed significant differences in chemical shifts in the published ^{1}H and ^{13}C NMR data of this substance and our results (vide supra), with the same solvent we used. For instance, the ^{13}C NMR signal for C-6″ at 96.4 ppm is more likely the C-8″ of the amentoflavone series. All correlations above-mentioned clearly indicate that the proposed structure isolated from *C. pyramidalis* requires revision.

For rings B and C of the second biflavonoid subunit, correlations in **2** were found for H−C(3″) and C(1‴), for H−C(2‴) and C(2″), C(6‴), C(3‴), and C(4‴), for H−C(3‴) and C(4‴), C(1‴), and C(5‴), for H−C(5‴) and C(3‴), C(4‴), and C(1‴), and for H−C(6‴) and C(2″), C(2‴), C(4‴), and C(5‴).

2,3-Dihydrorobustaflavone 5-methyl ether (**3**) was obtained as a yellow powder. Its spectral properties suggested the same biflavonoid type skeleton as compounds **1** and **2**. Low-resolution FAB$^+$-MS experiments showed the $[M + H]^+$ signal at *m*/*z* 555 in accord with the molecular formula of $C_{31}H_{22}O_{10}$. Its

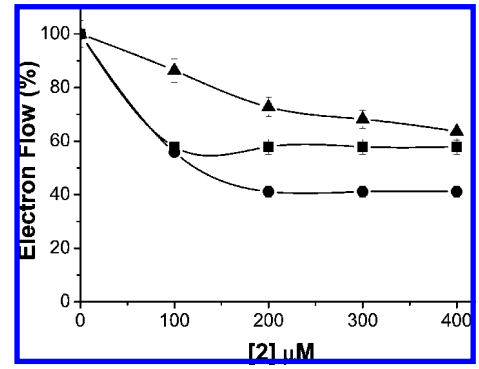

Figure 4. Effect of 2,3-dihydrorobustaflavone (**2**) on electron transport flow: basal (■); phosphorylating (●), and uncoupled (▲). Control = 100% = 760, 680, and 880 μequiv of e^-/mg of Chl/h, respectively. Each curve is the average of three replicates.

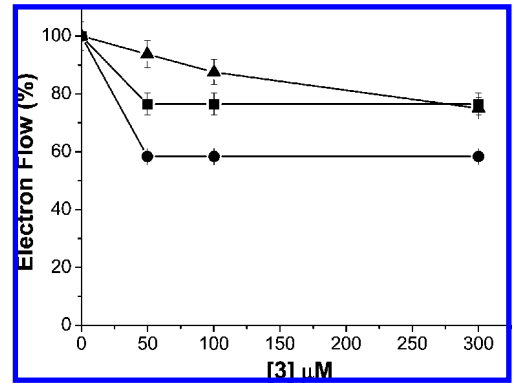

Figure 5. Effect of 2,3-dihydrorobustaflavone 5-methylether (**3**) on electron transport flow: basal (■); phosphorylating (●); uncoupled (▲). Control = 100% = 756, 533, and 355 μequiv of e^-/mg of Chl/h, respectively. Each curve is the average of three replicates.

NMR spectra (**Tables 2** and **3**) also showed similarities with compounds **1** and **2**; however, only one chelated OH group at δ(H) 13.46 (5″-OH) (**Table 2**) was observed. Three aliphatic resonances at δ(H) 5.36, 2.99, and 2.59, in combination with a C=O ^{13}C NMR resonance at δ 188.3, indicated the presence of a flavanone subunit. In both the flavanone and flavone subunits, the full set of HMBC correlations were obtained between CH_2(3) and C(4), C(1′), and C(2), between H−C(2′) and C(4′), C(2), C(6′), and C(6″), between H−C(5′) and C(4′), C(3′), and C(1′), and between H−C(6′) and C(4′), C(2), and C(2′), as well as between H−C(6) and C(5), C(7), C(8), and C(4a) and between H−C(8) and C(7), C(6), C(8a), and C(4a). A very important HMBC correlation was found between hydrogens of a methoxyl group (δH 3.76) with C(5) (δ163.7) which, as above-mentioned, correlated with H-(6). The only NOESY correlation with H−C(6) and the exaltation of the signal of this last group by irradiation of the methyl group in the NOE-1D experiment confirmed the position of the methoxyl group at C(5).

Two ^{1}H NMR resonances at δ 7.92 (2‴, 6‴) and 7.01 (3‴, 5‴) of **3** indicated a para-substituted aromatic B-ring in the second subunit. The interflavonoidal linkage was established through the HMBC correlation between H−C(2′) and C(6″). Other HMBC correlations between nuclei of the second subunit were observed: between H−C(3″) and C(2″), C(4″), C(4″a), and C(1‴), between H−C(8″) and C(8″a), C(4″a), C(6″), and C(7″), between H−C(2‴) and C(6‴) and C(4‴), between H−C(3‴) and C(4‴), C(5‴), and C(1‴), between H−C(5‴) and C(3‴), C(4‴), and C(1‴), and between H−C(6‴) and C(2‴), C(4‴), and C(2″).

Table 4. Effect of Biflavonoids on Electron Transport Flow: PSII, PSII from H_2O to SiMo, PSII from DPC to DCPIP, PSI from DCPIPred to MV, and $TMQH_2$ to MV

	PSII						PSI			
	H_2O to DCPIP		H_2O to SiMo		DPC to DCPIP		DCPIP to MV		$TMQH_2$ to MV	
compd	μequiv of e^- mg^{-1} of Chl h^{-1}	%	μequiv of e^- mg^{-1} of Chl h^{-1}	%	μM DCPIPred mg^{-1} of Chl h^{-1}	%	μequiv of e^- mg^{-1} of Chl h^{-1}	%	μequiv of e^- mg^{-1} of Chl h^{-1}	%
1										
0 μM	400 ± 20.0	100	311 ± 16.0	100	269 ± 13.5	100	2453	100	2629	100
100 μM	228 ± 11.4	57	311 ± 16.0	100	172 ± 8.6	89	2453	100	2629	100
200 μM	168 ± 8.0	43	156 ± 9.0	50	127 ± 9.0	35	2453	100	2629	100
300 μM	108 ± 5.0	29	156 ± 9.0	50	84 ± 4.2	9	2453	100	2629	100
2										
0 μM	400	100					2453 ± 127	100	2629 ± 131	100
50 μM	400	100					2355 ± 118	96	2629 ± 131	100
100 μM	400	100					1973 ± 99	74	2606 ± 131	98
200 μM	400	100					1894 ± 95	71	1928 ± 96	74
300 μM	400	100					1894 ± 95	71	1893 ± 95	72
3										
0 μM	400	100					2453	100	2629	100
100 μM	400	100					2453	100	2629	100
200 μM	400	100					2453	100	2629	100
300 μM	400	100					2453	100	2629	100

In the circular dichroism (CD) spectra of **2** and **3**, Cotton effects with a negative sign ($\pi\rightarrow\pi^*$ transition) at 287 and 290 nm and a positive sign ($n\rightarrow\pi^*$ transition) at 330 and 331 nm were observed, which indicated the absolute (*S*)-configuration at C(2) (*24*). On the basis of the above spectroscopic evidence, **2** and **3** were identified as 2(*S*)-2,3-dihydrorobustaflavone and 2(*S*)-2,3-dihydrorobustaflavone 5-methyl ether, respectively. This last natural product is novel in that it contains a methoxy group at position 5 of subunit I of the biflavonoid.

ATP Synthesis Inhibition by Biflavonoids 1−3. All biflavonoids isolated in this work displayed inhibition on ATP synthesis coupled to electron transport from water to MV in isolated freshly lysed intact spinach chloroplasts. It was observed that at increasing concentrations of biflavonoids, the synthesis of ATP decreased (**Figure 2**). The I_{50} values for **1**, **2**, and **3** were 44, 39, and 79 μM, respectively.

Effect of Biflavonoids 1−3 on Electron Transport Rate from Water to MV in Chloroplasts. To know the mechanism of inhibition of biflavonoids on ATP synthesis coupled to electron transport (basal, phosphorylating, and uncoupled), electron transport from water to MV was studied in freshly lysed spinach chloroplasts. We explored whether the effects on ATP synthesis could be inhibited by blockage of the electron transport within the thylakoid chain, by direct inhibition of the H^+-ATPase complex or by dissipation of the H^+ gradient, that is, uncoupling effect (*25*). **Figures 3**, **4**, and **5** show the effect of **1**, **2**, and **3** on chloroplast electron transport, respectively. The biflavonoids partially inhibited the three modes of electron flow, **1** being the most active electron transport flow inhibitor. The I_{50} value for uncoupled electron flow for **1** was 88 μM, which was 50% less active than its effect on ATP synthesis inhibition, suggesting that **1** may have another site of inhibition. It is well-known that light induces conformational changes of chloroplasts (measured by absorption change) related to energy conservation mechanisms as photophosphorylation, and both ATP formation and uncouplers diminish these conformational changes (*26*). We found that upon illuminated chloroplasts, **1** strongly inhibited uncoupled electron transport flow (50% at 88 μM) in the nonenergized state; however, **1** weakly inhibited basal electron transport rate, the energized state, by 22% at 88 μM. We propose that **1** senses different conformation changes in its target interaction in the chloroplasts when it is in different energized states (**Figure 3**). At 300 μM, biflavonoids **2** and **3** showed uncoupled electron transport flow inhibition by 32 and 25%, respectively. These biflavonoids, **2** and **3**, were less active than **1** (**Figures 4** and **5**). Overall results indicate that **1−3** act as Hill reaction inhibitors, demonstrated in the photoreduction of an electron acceptor (MV) at the expense of water, which is oxidized to oxygen.

To localize the target of **1−3** on the thylakoid electron transport chain, effects on partial reactions of PSII and PSI electron transport were determined using appropriate artificial electron donors, electron acceptors, and electron transport inhibitors (*27, 28*). **Table 4** shows that **1** had no effect on PSI determined in chloroplasts. However, it inhibited PSII electron flow from water to oxidized DCPIP, as well as the partial reactions from water to SiMo and from DPC to DCPIP, with I_{50} values of 121, 181, and 154 μM, respectively. The partial inhibition of the reaction with SiMo as an electron acceptor indicated that **1** partially inhibited uncoupled PSII electron transport at the oxygen evolving complex (OEC) system, the water splitting enzyme (*9*). Furthermore, the partial reaction from DPC to DCPIP, assayed using Tris-washed thylakoids, was also inhibited. These results indicate that the interaction and inhibition site of **1** is located between P_{680} and Q_A of the PSII electron transport chain, because reduced DPC donates electrons to P_{680} (*12*). Therefore, **1** interacts with PSII from span of OEC to the reaction center. Compound **2** did not affect PSII. However, it partially inhibited PSI from reduced DCPIP (with ascorbate) to MV and from $TMQH_2$ to MV. These results are indicative that the action site for **2** was located on PSI. To determine its inhibition site on PSI, its effect on the partial reaction from PMS reduced with ascorbate to MV on treated thylakoids with KCN was assayed. It was found that **2** did not inhibit this partial reaction (data not shown). Therefore, the interaction and inhibition target of **2** is located in the span of the electron transport chain from the Cyt b_6f complex to PC. Compound **3** did not have any effect on PSII, PSI, or PSI measured from $TMQH_2$ to MV; however, it may act as an energy transfer inhibitor.

To corroborate findings on the interaction site of **1** at PS II, chlorophyll *a* fluorescence kinetics were determined in freshly lysed chloroplasts; one set of samples was incubated for 5 min in the dark with 10 μM DCMU, and a second set of samples of chloroplasts was incubated with 0.8 M Tris for 30 min at 4 °C. Both preparations were used as positive controls. Chlorophyll

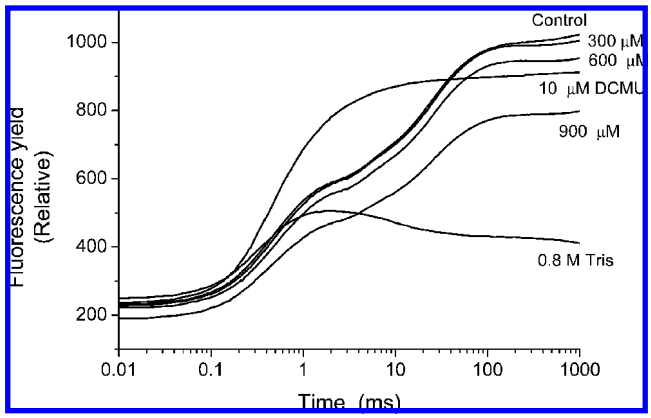

Figure 6. Induction curves of fluorescence of chlorophyll *a* of thylakoids treated with 10 μM DCMU, 0.8 M Tris, and increasing concentrations of **1**. Results are the average of three replicates.

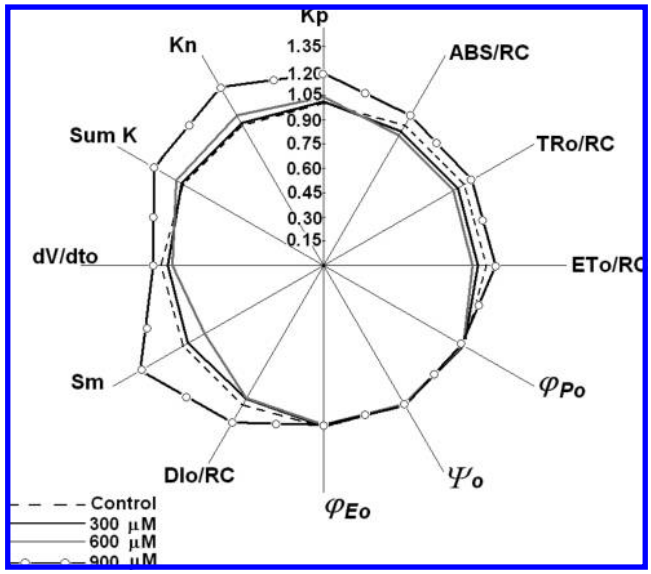

Figure 7. Spider plot showing some JIP test parameters affected by 300, 600, and 900 μM **1**; comparison of the corresponding means (%). Results are the average of three replicates.

a fluorescence can be regarded as an intrinsic probe of the photosynthetic system and the intensity of the fluorescence as a direct measure of the PSII activities. In the fluorescence induction curve (**Figure 6**) the control thylakoids exhibited a polyphasic O-J-I-P transient (*3*). Addition of herbicide DCMU, used as positive control, resulted in a fast rise of fluorescence yield during the first 2 ms of illumination, transforming the regular O-J-I-P sequence into an O-J curve (**Figure 6**) (*3*). The other positive control were the thylakoids treated with 0.8 M Tris, which causes loss of electron donation ability and loss of Mn^{2+} complex at the same rate that it inhibits O_2 evolution (**Figure 6**) (*29, 30*). Different photosynthetic parameters of fluorescence kinetics of PSII from **Figure 6** were used to build **Figure 7**, which shows the specific fluxes that were increased until <20% at 900 μM **1**, such as the effective antenna size (ABS/RC) of an active reaction center (RC), the maximal rate by which an excitation is trapped by the RC (TRo/RC), the electron transport in an active RC (ETo/RC), and the non-photochemical energy dissipation per reaction center (DI_0/RC). The de-excitation constants (K_p, K_n) and their sum K, the total electron transport carriers per RC (Sm), and the specific activity of primary photochemistry (dV/dt_0) increased, too, but in a major proportion that the specific fluxes, whereas the yields or flux ratios (φ_{P0}, Ψ_0, and φ_{E0}) stayed constant at 900 μM **1** (**Figure 7**). However, at 300 and 600 μM all parameters above-mentioned remained quasi-unaffected. These results indicate that the reaction centers partially lost their capacity to capture excitons when thylakoids were treated with **1**. The increase in K_n value and in DI_0/RC shows the toxicity of **1** on PSII at 900 μM. On the other hand, φ_{P0} indicates the probability (at $t = 0$) that a trapped exciton moves an electron into the electron transport chain beyond Q_A^-, together with the quantum yield of electron transport, remained constant, which suggested that **1** interacts with PSII, decreasing the number of active reaction centers at 900 μM. Thus, **1** acts by inhibiting the PSII at the reaction centers level.

Table 5. Effect of Increasing Concentrations of Biflavonoids and Ammonium Chloride on Mg^{2+}-ATPase Activity

compd	μM P mg^{-1} of Chl h^{-1}	activity (%)
1		
0 μM	116 ± 14	100
100 μM	88 ± 14	76
200 μM	88 ± 14	76
300 μM	88 ± 14	76
2		
0 μM	116 ± 6	100
100 μM	61 ± 3	53
200 μM	54 ± 3	47
300 μM	39 ± 2	34
3		
0 μM	116 ± 6	100
100 μM	73 ± 4	63
200 μM	51 ± 3	44
300 μM	23 ± 2	20
NH_4Cl		
0 mM	116 ± 6	100
1 mM	239 ± 12	206
3 mM	278 ± 14	240
6 mM	144 ± 7	124

Effect of Biflavonoids 1−3 on Mg^{2+}-ATPase Membrane. To determine if **1**−**3** interact with the H^+-ATPase complex in inhibiting photophosphorylation, their effect on Mg^{2+}-ATPase activity associated with the thylakoid membranes was investigated. **Table 5** shows that increasing concentrations of ammonium chloride enhanced the Mg^{2+}-ATPase activity, as uncouplers do (*4*), which is used as positive control, and increasing concentrations of **1**, **2**, and **3** inhibited the Mg^{2+}-ATPase activity. The overall results indicate that **1**−**3** act as energy transfer inhibitors, **3** being the most active (80% of inhibition at 300 μM) with similar values of percentage of inhibition in ATP synthesis; therefore, **3** acts only as an energy transfer inhibitor. Compound **2** showed 66% inhibition of the Mg^{2+}-ATPase activity at the same concentration (300 μM), indicating that it partially acts as both a Hill reaction inhibitor and an energy transfer inhibitor. **1** behaved as the least active in affecting the Mg^{2+}-ATPase (24% of inhibition at 300 μM); therefore, it acts as a potent Hill reaction inhibitor. The present study suggests that biflavonoids **1** and **2** isolated from *S. lepidophylla* inhibit PSII when they act as Hill reaction inhibitors and they inhibit the H^+-ATPase of the chloroplasts when they act as energy transfer inhibitors; compound **3** acts only as an energy transfer inhibitor. Further studies will be required to demonstrate that inhibition of **1**−**3** in chloroplasts is the way in which they act as allelochemicals.

ACKNOWLEDGMENT

We thank R. I. del Villar, A. Acosta, G. Duarte, M. Guzmán, and M. Gutiérrez for spectroscopic assistance and Dr. R. Bye for identification of the vegetal species. This research was taken in part from the B.Sc. thesis of M.G.R.

Supporting Information Available: ^{1}H and ^{13}C NMR and HMBC spectra of compound **1** and HMBC spectra of compounds **2** and **3**. This material is available free of charge via the Internet at http://pubs.acs.org.

LITERATURE CITED

(1) Martínez, M. *Las Plantas Medicinales de México*, 6th ed.; Ediciones Botas: México City, Mexico, 1989; pp 124−125.
(2) Zembower, D. E.; Lin, Y. M.; Flavin, M. T.; Chen, F. C.; Korba, B. E. Robustaflavone, a potential non-nucleoside anti-hepatitis B agent. *Antiviral Res.* **1998**, *3*, 81–88.
(3) Strasser, R. J.; Srivastava, A.; Govindjee. Polyphasic chlorophyll *a* fluorescence transients in plants and cyanobacteria. *Photochem. Photobiol.* **1995**, *61*, 32–42.
(4) Mills, J. D.; Mitchell, P.; Schurmann, P. Modulation of coupling ATPase activity in intact chloroplasts. *FEBS Lett.* **1980**, *191*, 144–148.
(5) Morales-Flores, F.; Aguilar, M. I.; King-Díaz, B.; de Santiago-Gómez, J. R.; Lotina-Hennsen, B. Natural diterpenes from *Croton ciliatoglanduliferus* as photosystem II and photosystem I inhibitors in spinach chloroplasts. *Photosynth. Res.* **2007**, *91*, 71–80.
(6) Strain, H. H.; Cope, T.; Svec, M. A. Analytical procedures for the isolation, identification, estimation and investigation of the chlorophylls. *Methods Enzymol.* **1971**, *23*, 452–466.
(7) Dilley, R. A. Ion transport (H^{+}, K^{+}, Mg^{2+} exchange phenomena). *Methods Enzymol.* **1972**, *24*, 68–74.
(8) Izawa, S.; Hind, G. The kinetics of the pH rise in illuminated chloroplasts suspensions. *Biochim. Biophys. Acta* **1967**, *143*, 377–390.
(9) Guiaquinta, R. T.; Dilley, R. A. A partial reaction in photosystem II: reduction of silicomolybdate prior to the site of dichlorophenyldimethyl-urea inhibition. *Biochim. Biophys. Acta* **1975**, *387*, 288–305.
(10) Armstrong, J. McD. The molar extinction coefficient of 2,6-dichlorophenol indophenol. *Biochim. Biophys. Acta* **1964**, *86*, 194–197.
(11) Yamashita, T.; Horio, T. Non-cyclic photophosphorylation by spinach grana treated with 0.8 M tris buffer. *Plant Cell Physiol.* **1968**, *9*, 268–284.
(12) Vernon, L. P.; Shaw, E. R. Photoreduction of 2,6-dichlorophenol by diphenylcarbazide: a photosystem 2 reaction catalyzed by Tris-washed chloroplasts and subchloroplasts fragments. *Plant Physiol.* **1969**, *44*, 1645–1649.
(13) Ouitrakul, R.; Izawa, S. Electron transport and photophosphorylation in chloroplast a function of electron-acceptor 2. Acceptor-specific inhibition by KCN. *Biochim. Biophys. Acta* **1973**, *305*, 105–118.
(14) Izawa, S.; Krayenhof, R.; Ruuge, E. K.; DeVault, D. The site of KCN inhibition in the photosynthetic electron transport pathway. *Biochim. Biophys. Acta* **1973**, *314*, 328–339.
(15) Izawa, S.; Pan, R. L. Photosystem I electron transport and phosphorylation supported by electron donation to the plastoquinone region. *Biochem. Biophys. Res. Commun.* **1978**, *83*, 1171–1177.
(16) Panda, D.; Rao, D. N.; Sharma, S. G.; Strasser, R. J.; Sarkar, R. K. Subemergence effects on rice genotypes during seedling stage: Probing of subemergence driven changes of photosystem 2 by chlorophyll *a* fluorescence induction O-J-I-P transients. *Photosynthetica* **2006**, *44*, 69–75.
(17) Sumner, J. B. Scientific apparatus and laboratory methods. A method for the colorimetric determination of phosphorous. *Science* **1944**, *100*, 413–415.
(18) Qasim, M. A.; Roy, S. K.; Kamil, M.; Ilyas, M. Phenolic constituents of Selaginellaceae. *Indian J. Chem.* **1985**, *24B*, 220.
(19) Chari, V. M.; Ilyas, M.; Wagner, H.; Neszmélyi, A.; Chen, F. C.; Chen, L. K.; Lin, Y. C.; Lin, Y. M. ^{13}C NMR spectroscopy of biflavonoids. *Phytochemistry* **1977**, *16*, 1273–1278.
(20) Markham, R. K.; Sheppard, C.; Geiger, H. ^{13}C NMR studies of some naturally occurring amentoflavone and hinokiflavone biflavonoids. *Phytochemistry* **1987**, *26*, 3335–3337.
(21) Lin, L. C.; Kuo, Y. C.; Chou, C. J. Cytotoxic biflavonoids from *Selaginella delicatula*. *J. Nat. Prod.* **2000**, *63*, 627–630.
(22) Joly, M.; Haag-Berrurier, M.; Anton, R. La 5′-méthoxybilobétine,une biflavone extraite du *Ginkgo biloba*. *Phytochemistry* **1980**, *19*, 1999–2002.
(23) Bahia, M. V.; Dos Santos, J. B.; David, J. P.; David, J. M. Biflavonoids and other phenolics from *Caesalpinia pyramidalis* (Fabaceae). *J. Braz. Chem. Soc.* **2005**, *16*, 1402–1405.
(24) Gaffield, W. Circular dichroism, optical rotatory dispersion and absolute configuration of flavanones, 3-hydroxyflavanones and their glycosides: determination of aglycone chirality in flavanone glycosides. *Tetrahedron* **1970**, *26*, 4093–4108.
(25) Good, N. E.; Izawa, S.; Hind, G. Uncoupling and energy transfer inhibition in photophosphorylation. In *Current Topics in Bioenergetics*; Sanadi, D. R., Ed.; Academic Press: New York, 1981; Vol. 1, pp 75−112.
(26) Dilley, R. A.; Vernon, L. P. Light-induced conformational changes of chloroplasts produced by high energy intermediates of photophosphorylation. *Biochem. Biophys. Res. Commun.* **1964**, *15*, 473–478.
(27) Allen, J. F.; Holmes, N. G. Electron transport partial reactions. In *Photosynthesis, Energy Transduction. A Practical Approach*; Hipkins, M. F., Baker, N. R., Eds.; IRL Press: Oxford, U.K., 1986; pp 103−141.
(28) Saha, S.; Ouitrakul, R.; Izawa, S. Electron transport and phosphorylation in chloroplasts as a function of the electron acceptor. *J. Biol. Chem.* **1971**, *246*, 3204–3209.
(29) Rickert, K. W.; Sears, J.; Beck, W. F.; Brudvig, G. W. Mechanism of irreversible inhibition of O_2 evolution in photosystem II by tris(hydroxymethyl)aminomethane. *Biochemistry* **1991**, *30*, 7888–7894.
(30) Strassser, R. J.; Tsimilli-Michael, M.; Srivastava, A. Analysis of chlorophyll *a* fluorescence transient. In *Chlorophyll Fluorescence: A Signature of Photosynthesis*; Papageorgiou, G. C., Govindjee, Eds.; Kluwer Academic Publishers: Dordrecht, The Netherlands, 2004; Chapter 12, pp 321−362.

Received for review April 2, 2008. Revised manuscript received June 11, 2008. Accepted June 17, 2008. We thank Dirección General de Asuntos del Personal Académico de la UNAM (DGAPA) for financial support (PAPIIT IN 211807 and 205806).

JF8010432